JOURNAL OF MATERIALS SCIENCE **40** (2005) 621–627

The effect of metallocene-catalyzed linear low-density polyethylene on the physicomechanical properties of its film blends with low-density polyethylene

M. J. CRAN, S. W. BIGGER*
School of Molecular Sciences, Victoria University of Technology, Werribee Campus, P.O. Box 14428, MCMC, Melbourne, 8001, Australia
E-mail: Stephen.bigger@vu.edu.au

Films comprising a metallocene-catalyzed linear low-density polyethylene (mLLDPE) blended with either of two different low-density polyethylene (LDPE) materials were prepared. The physicomechanical, optical and melt flow properties of the films were measured. A novel adaptation of conventional radar plots was used to process the acquired data to identify the level at which mLLDPE should be incorporated in either of the LDPEs to produce optimal overall properties. In general, the addition of mLLDPE to LDPE improved most of the properties considered and the LDPE material having the higher polydispersity produced blends having superior properties. A level of mLLDPE of between 20–30% (w/w) was required in order to achieve optimization.

1. Introduction

Linear low-density polyethylene (LLDPE) is produced *via* the copolymerisation of ethylene with a small amount of an α-olefin. Short side chains on the ethylene backbone are thus introduced [1] which causes LLDPE to have a melting temperature between that of low-density polyethylene (LDPE, m.p. range 108–115°C) and high-density polyethylene (HDPE, m.p. range 130–135°C) [2]. It is claimed that the branches in LLDPE affect its crystallinity [3, 4] and crystalline melting point [1, 5] and improve other properties such as stiffness [6], tensile strength [7, 8], chemical resistance [3, 9], tear strength [10], fracture toughness [11, 12] and impact toughness [13, 14].

The type and amount of α-olefin co-monomer determines the physical and mechanical properties of LLDPE [8, 15–17]. Variations in the co-monomer content, reactor conditions and catalysts used can improve tensile strength, tear resistance and melt viscosity [10]. Several studies have suggested that the impact toughness of LLDPE is due to the presence of a second rubbery phase resulting from the short-chain branching [11, 12, 14], although another study [13] suggests that the improved toughness is independent of the amount of this second phase and that a rubber-toughening effect is not responsible for the observed impact behaviour.

The processability of conventional LLDPE is different to that of LDPE [6, 18, 19] and therefore film blends of these materials may require different processing conditions compared to pure LDPE films [20]. For resins with the same melt flow index, LLDPE is tougher than LDPE and therefore thinner films of LLDPE can have equivalent mechanical properties to thicker LDPE films [18]. The production of films from pure LDPE presents minimal difficulties and good bubble stability is maintained throughout the extrusion process due to the long chain branching content of the LDPE [18]. The high melt viscosity of pure LLDPE, however, can cause melt fracture if conventional LDPE extrusion equipment is used [6, 21]. Increasing the extrusion temperatures and widening the die gap can reduce the occurrence of melt fracture but this reduces the bubble stability [21].

Blends of conventional LLDPE with LDPE have been widely reported in the literature [3, 6, 7, 21–29] and it has been suggested that the addition of LLDPE significantly improves various properties of LDPE. For instance, the addition of LLDPE to LDPE to form a binary blend enhances the crystallisation rate and improves properties such as impact strength, optical clarity, environmental stress-cracking resistance as well as resistance to thermal embrittlement [7]. Furthermore, blending LLDPE with LDPE can result in significant improvements in film qualities including toughness, mechanical properties and optical properties as well as increasing the melt tension and the film bubble stability [3, 26]. The elongation viscosity of blends of

*Author to whom all correspondence should be addressed.

LDPE/LLDPE is shown to vary in proportion to the LDPE content and this is an important factor when modelling processes such as blow moulding and film blowing [25]. The toughness of LDPE and its bubble stability during tubular extrusion blowing are also improved by the addition of LLDPE [21, 23].

Blends of LLDPE with LDPE have been found to be miscible in the melt and do not segregate into separate phases provided they are cooled quickly from the melt [22]. The slow cooling of molten LDPE/LLDPE blends, however, results in the formation of independent crystalline phases that can be associated with the two constituent polymers [3, 27, 30]. The melting behaviour of conventional LLDPE and blends with LDPE has been widely studied [3, 13, 27, 30–37]. In most cases the melting endotherms show two distinct melting peaks corresponding to constituent polymers [27]. It has been suggested that the blend is volume filled by LLDPE and that LDPE crystallises separately within the crystalline domains of the LLDPE component [27].

The use of metallocene catalysts in the production of LLDPE results in polymers with different properties compared to conventional LLDPE resins made using similar co-monomers [38–43]. The short-chain branching in metallocene-catalyzed LLDPE (mLLDPE) is more evenly distributed along the PE chain and typical resins are produced with much lower densities than conventional LLDPE [1, 42, 43]. Film-grade mLLDPE has improved impact strength [44], tensile properties and optical clarity [41] compared with conventional LLDPE. It also exhibits lower melting temperatures [43] and improved heat seal strength [39] than conventional LLDPE.

It has been found that blending mLLDPE with LDPE produces a film that has improved properties compared with the pure LDPE film [44–48] and that such blends can also be processed significantly better than blends of conventional LLDPE with LDPE [44]. In view of the potential of mLLDPE to enhance the physicomechanical properties of LDPE the current paper examines certain binary blends of mLLDPE with LDPE in order to identify any blends that have optimal and desirable characteristics.

2. Experimental section

2.1. Materials

Two LDPE resins (LDPE1 and LDPE2) and one mLLDPE resin (with butene comonomer) were used to prepare the blends that were studied. The characteristic properties of these resins are given in Table I.

TABLE I Characteristic properties of LDPE1, LDPE2 and mLLDPE resins

Resin	Density/ kg m^{-3}	MFI/ dg min^{-1}	m.p./°C	MW/ Dalton	PD
LDPE1	921	0.2	109	20,000	8.0
LDPE2	921	0.9	111	14,000	11
mLLDPE	901	0.6	93	30,000	2.3

2.2. Blend preparation

Blends containing 10, 20, 50, 75 and 90% (w/w) mLLDPE with LDPE1 or LDPE2 were prepared by dry blending the polymers for 15 min. Each blend was then compounded in a Gonninan extrusion compounder and the extrudate was immediately cooled in a water bath, dried and pelletised.

A sample of each compounded blend was collected for film extrusion and physical property measurements. Each of the compounded blends, as well as each of the respective resins, was blown into a film using a Glouchester film extruder. The screw speed used in the production of each film was 90 rpm except for those comprising 50, 75, 90 and 100% (w/w) mLLDPE, where the speed was 50 rpm to account for the increased viscosity of these melts. The die gap for each film was 1 mm except for the 50, 75, 90 and 100% mLLDPE films, which was 2 mm.

2.3. Measurement of physical properties

The melt flow index (MFI) of each blend of mLLDPE with LDPE1 or LDPE2 was measured using a Davenport melt rheometer in accordance with ASTM method D-1238 using both a 2.16 kg load and a 21.6 kg load, at a melt temperature of 190°C. Density measurements were performed in accordance with ASTM method D-2839.

2.4. Measurement of film properties

Tensile testing of the film samples was performed using an Instron tensile testing machine in accordance with ASTM method D-882. A crosshead speed of 500 mm min^{-1} and a sampling rate of 10 points s^{-1} were used. The impact strength was determined using a free-falling dart impact tester in accordance with ASTM method D-1709. The tear resistance measurements were conducted using an Elmendorf tear strength tester in accordance with ASTM method D-1922. The percent haze of each film sample was measured in accordance with ASTM method D-1003 using a Gardner haze meter and the percent gloss of each sample was measured in accordance with ASTM method D-2457 using a Pacific Scientific Glossgard II 45° gloss meter.

Tensile strength and tear strength tests were performed in both the machine direction (MD) and transverse direction (TD) for each sample of film.

2.5. Theoretical manipulation of data—radar plots

The physicomechanical and optical data can be most conveniently handled simultaneously by means of a "radar" plot in which these parameters are plotted on a percentage scale on separate radial axes that issue outwards from an origin and the axes are equiangular with respect to each other. In the current work the radials on each radar plot are calibrated in 20% increments with zero being at the center of the plot and 100% at the outermost limit. Standardization of each quantity appearing on the plot was achieved by, firstly, identifying

the maximum value of that quantity that was observed over all experiments, and secondly, expressing the corresponding datum as a percentage of that value. The haze data are represented on the radar plots as the difference between the maximum percent haze value and the particular percent haze value, in order to provide a quantity whose value increases as the haze decreases. Thus, an improvement in the overall properties of a material will be indicated on the radar plot by dilation of the resultant polygon towards the outer extremities of the plot and a concomitant increase of the area of the polygon.

The total area of a polygon on a radar plot is the sum of the areas of its triangular segments.

The area, A_i, of the ith triangular segment defined by the ordinate (r_i, r_{i+1}, 0) on a radar plot having n such segments is given by Equation 1:

$$A_i = \sum_{i}^{n-1} 1/2\,[r_i r_{i+1} \sin(2\pi/n)] \tag{1}$$

Since $r_n = r_1$, then the total area, A_T of the polygon is given by:

$$\begin{aligned} A_T &= A_n + \sum_{i=1}^{n-1} A_i \\ &= 1/2\,[r_{n-1} r_1 \sin(2\pi/n)] \\ &\quad + \sum_{i=1}^{n-1} 1/2\,[r_i r_{i+1} \sin(2\pi/n)] \end{aligned} \tag{2}$$

The melt flow ratio (MFR) parameter that is derived from MFI and hence reflects processability [19, 49], was not included on the radar plots as this parameter can be plotted as a function of the blend composition and superimposed on a graph of the radar plot area versus composition in order to identify an optimal blend composition. Such a blend would presumably have optimal physicomechanical and optical properties along with optimal processability.

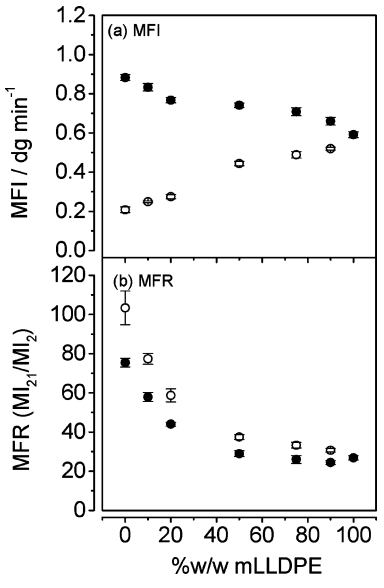

Figure 1 Plots of: (a) MFI versus blend composition and (b) MFR versus blend composition for mLLDPE/LDPE1 blends (open circles) and mLLDPE/LDPE2 blends (filled circles).

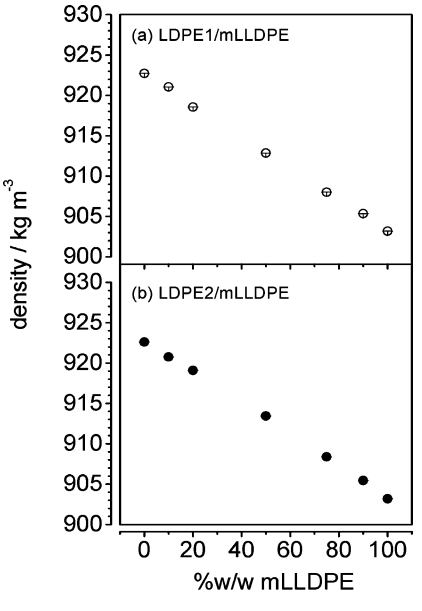

Figure 2 Plots of density versus blend composition for (a) mLLDPE/LDPE1 blends and (b) mLLDPE/LDPE2 blends.

3. Results and discussion

3.1. Physical properties

The MFI of a polymer is related to its molecular weight distribution and is often used to characterize processability [19, 49]. A plot of MFI versus blend composition for LDPE1/mLLDPE and LDPE2/mLLDPE blends is shown in Fig. 1a. The MFI for blends of mLLDPE with LDPE1 increases approximately linearly whereas the MFI for blends with LDPE2 show a downward trend over the range of compositions. A plot of the corresponding MFR (MI_{21}/MI_2) versus blend composition for each of these blends is shown in Fig. 1b. From this plot it is evident that the MFR for each of the blends is less than additive and that the MFR of pure mLLDPE is significantly lower than that of pure LDPE1 or LDPE2. These data are consistent with the notion that metallocene-catalyzed PE (mPE) resins have narrow molecular weight ranges which is reflected by their low MFR values [39, 41, 43]. Furthermore, the data in Fig. 1b suggest that the polydispersity of LDPE1 is greater than that of LDPE2.

The density of PE is a function of the type and level of long and short-chain branching within the polymer [50]. Fig. 2 shows plots of density versus blend composition for blends of mLLDPE with LDPE1 or LDPE2. From these plots it can be seen that the density of the blend is additive with respect to the blend composition. Such linearity has been shown to be the case for a number of polyethylene blends [20, 51–53] and suggests that the presence of one type of crystal in the blend has little effect on the ability of the other species to crystallise from the melt [20]. The density of pure mLLDPE component is lower than conventional LLDPE resins which is another characteristic property of mPE resins [39, 42, 43].

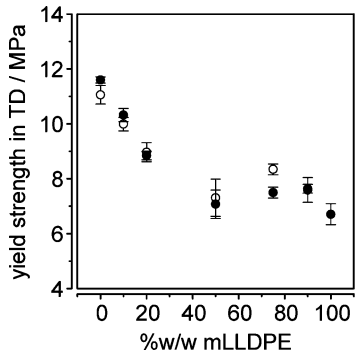

Figure 3 Plot of yield strength in TD versus blend composition for mLLDPE/LDPE1 blends (open circles) and mLLDPE/LDPE2 blends (filled circles).

3.2. Slow-rate, small deformation mechanical properties

The yield strength in the TD as a function of composition for the blends of mLLDPE with LDPE1 or LDPE 2 is shown in Fig. 3. From this plot it is evident that the yield strength decreases with increasing levels of mLLDPE from about 11 to 7 MPa, and that this decrease is non-linear. In contrast, the yield strength of the film blends of conventional LLDPE with LDPE generally increases with the addition of LLDPE [26], which may be due to the heterogeneous short-chain branching distribution of LLDPE [7]. In the current work, there was no yield strength measurable in the MD of any of the 100% (w/w) films or, indeed, the blends. This has also been shown to be the case for conventional LLDPE/LDPE film blends [22, 54].

Plots of the break strength versus blend composition for each blend in the MD and TD of the film are shown in Fig. 4. In the MD (Fig. 4a), there is no significant variation in the break strength up to and including levels of ca. 50% (w/w) mLLDPE in either of the film blends. Furthermore, the values of the MD break strength in this range are similar for both of the blends, which may be attributable to a similar extent of alignment of the chains in each blend. For levels above 50% (w/w) mLLDPE, it is not clear whether this trend continues. However, in the TD (Fig. 4b) the variation in break strength appears to follow an upward trend across the entire composition range. There is also a significant increase (ca. 25%) in break strength in the TD after the addition of ca. 10% (w/w) mLLDPE. For film blends of conventional LLDPE with LDPE, the break strength is shown to decrease with increasing levels of LLDPE [21].

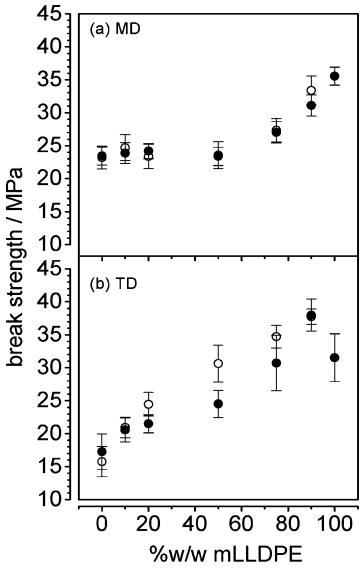

Figure 4 Plots of break strength versus blend composition for mLLDPE/LDPE1 blends (open circles) and mLLDPE/LDPE2 blends (filled circles) in: (a) MD and (b) TD.

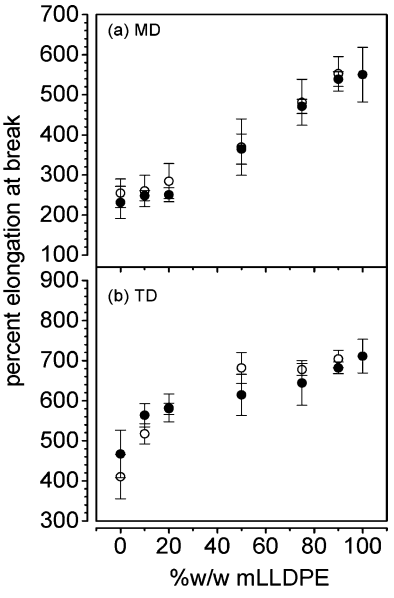

Figure 5 Plots of percent elongation at break versus blend composition for mLLDPE/LDPE1 blends (open circles) and mLLDPE/LDPE2 blends (filled circles) in: (a) MD and (b) TD.

The percent elongation at break versus composition in the film blends is shown in Fig. 5. In the MD of the film (Fig. 5a), the elongation at break increases with increasing mLLDPE in the blend with the most significant increase occurring above levels of ca. 20% (w/w) mLLDPE. In the TD of the film (Fig. 5b), the elongation values are numerically much greater than those corresponding to the MD and the increase in these values follows an immediate upward trend similarly to the case of the break strength data. In contrast, the elongation values for conventional LLDPE/LDPE blends have been shown to either decrease or increase only slightly with blend composition [21].

3.3. Fast-rate, large deformation mechanical properties

The dart impact test is a measure of the shock resistance of a film sample [21, 41, 43]. A plot of the dart impact strength versus blend composition for the film blends is shown in Fig. 6. The 100% (w/w) mLLDPE film has a much higher (ca. 90%) dart impact strength than either 100% (w/w) LDPE1 or 100% (w/w) LDPE2. The increase in dart impact strength with increased levels of mLLDPE is non-linear and there is a significant improvement in this property at levels above ca. 10% (w/w) mLLDPE [41]. The increase observed beyond this level may be due to the homogeneity of the molecular structure of the mLLDPE [41, 43]. Studies of

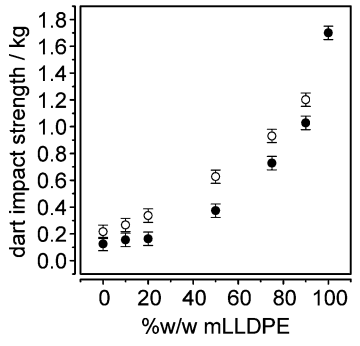

Figure 6 Plot of dart impact strength versus blend composition for mLLDPE/LDPE1 blends (open circles) and mLLDPE/LDPE2 blends (filled circles).

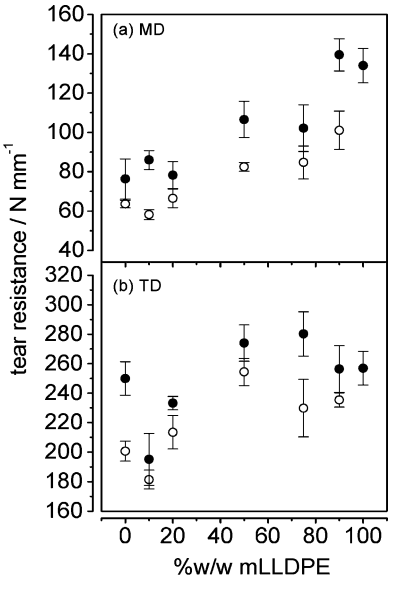

Figure 7 Plots of tear resistance versus blend composition for mLLDPE/LDPE1 blends (open circles) and mLLDPE/LDPE2 blends (filled circles) in: (a) MD and (b) TD.

conventional LLDPE/LDPE blends [21] do not show as significant an increase in dart impact strength over the range of compositions as that observed in the present work.

It is interesting to note that this fast-rate technique is capable of differentiating between the two LDPE materials insofar as there is a significant difference between both of the blends that can be detected at each of the compositions studied. The ability of this technique to differentiate between the two LDPE materials may be explained on the basis that dart impact strength is relatively independent of film orientation [55] and thus this test will reflect molecular structural properties without being influenced by the manner in which the sample has been produced.

A plot of tear resistance versus blend composition for both blends is shown in Fig. 7. In the MD (Fig. 7a), the tear resistance of both blends shows a similar upward trend with increasing mLLDPE content. In all cases, the tear resistance of the LDPE2 blend in the MD remains greater than that of the LDPE1 blend across the entire composition range which is to be expected due to the higher polydispersity of the LDPE2 [56].

In the TD (Fig. 7b) the scatter in the data make it difficult to identify any trend. Nonetheless, the observation can be made that the overall tear strength in the TD is greater than the corresponding tear strength in the MD at all compositions. Clearly, this is to be expected due to orientation effects resulting from the film blowing process [55, 56]. Furthermore, the superior tear strength of the LDPE1 compared with the LDPE2 is more apparent from the 100% (w/w) LDPE data obtained from TD experiments (Fig. 7a), than from the MD experiments (Fig. 7b).

In contrast, blends of conventional LLDPE with LDPE are reported to show a less than additive decrease in the MD tear resistance with increasing LLDPE content [6, 7, 21]. The structural differences between conventional LLDPE and mLLDPE are a possible reason for the behaviour observed elsewhere [39, 43] and that observed in the current work.

3.4. Optical properties

Fig. 8 shows plots of the percent haze and the percent gloss versus composition for both of the blends. From this plot it can be seen that the haze (Fig. 8a) increases to a maximum of ca. 9% at a blend composition of ca. 50% (w/w) LDPE1. This cloudiness in the film may be due to melt fracture that occurs in the blend as a result of some blend incompatibility [21]. The blends of mLLDPE with LDPE2 have overall less haze than the blends involving LDPE1, and have a maximum of ca. 6% haze. The blend containing LDPE2 shows a dramatic decrease in percent haze to ca. 3% at levels of mLLDPE greater than ca. 30% (w/w) whereas the blend containing LDPE1 persists at a high level of haze beyond that composition. The behaviour of the blend containing LDPE2 is comparable to that exhibited in blends of conventional LLDPE with LDPE which show a significant reduction in haze [21] and improved film clarity [6] with increased levels of LLDPE. The 100% (w/w) mLLDPE film exhibits the lowest haze and this reflects a characteristic property of mPE films resulting from their low crystallinity [41, 43].

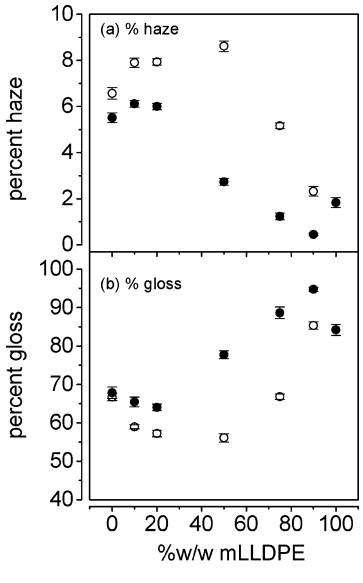

Figure 8 Plots of: (a) percent haze versus blend composition and (b) percent gloss versus blend composition for mLLDPE/LDPE1 blends (open circles) and mLLDPE/LDPE2 blends (filled circles).

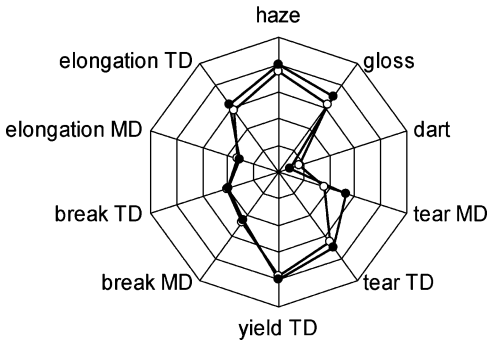

Figure 9 Radar plots of blends containing 10% (w/w) mLLDPE in LDPE1 (open circles) and LDPE2 (filled circles).

The plots of the percent gloss data (Fig. 8b) complement those data obtained for the percent haze insofar as blends that possess a high percent haze have a correspondingly low percent gloss and the optimal blend composition appears to be close to 30% (w/w) mLLDPE as previously indicated. The 100% (w/w) mLLDPE film has a gloss of ca. 95% that indicates its superior optical properties [41, 43].

3.5. Radar plots

Figs 9 and 10 show radar plots for the mLLDPE/LDPE1 and mLLDPE/LDPE2 systems at 10% (w/w) and 20% (w/w) mLLDPE respectively. The plots reveal that these systems have in general good haze, gloss, TD yield, and tear strength, but have relatively low dart impact strengths. The latter arises as a result of the normalization process used to obtain the dart impact data where the maximum dart impact was observed to be that corresponding to 100% (w/w) mLLDPE. At blend compositions in the range appropriate for, say, possible commercial films the level of mLLDPE would be much lower than this. Thus an arbitrary value of the maximum dart impact would be considerably lower and so the percent dart impact strengths would be correspondingly higher. In any case, the arbitrary nature of the choice in will not affect the overall comparisons between the blends so long as this value remains constant within the analyses.

The differences between the LDPE1 and LDPE2 constituents are relatively small across most properties represented on the radar plot at 10% (w/w) mLLDPE (see Fig. 9). On the other hand, more noticeable differences between these two materials can be seen at the higher

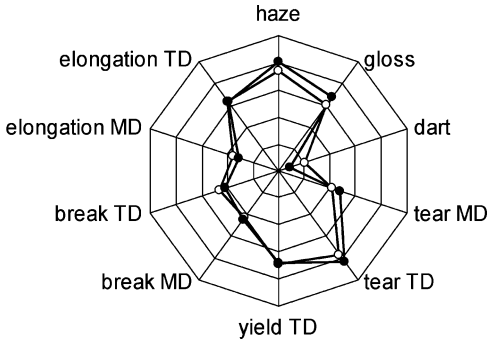

Figure 10 Radar plots of blends containing 20% (w/w) mLLDPE in LDPE1 (open circles) and LDPE2 (filled circles).

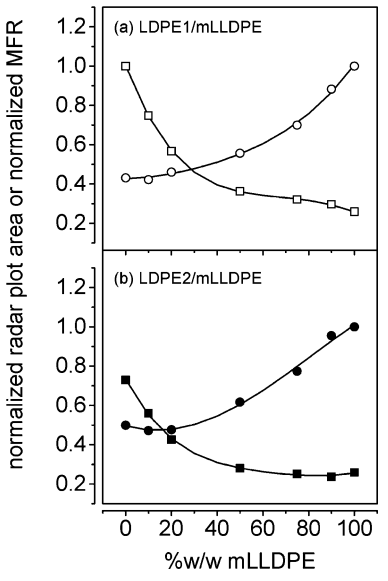

Figure 11 Plots of: (a) normalized radar plot area (open circles) and normalized MFR (open squares) versus blend composition for mLLDPE/LDPE1 blends and (b) normalized radar plot area (filled circles) and normalized MFR (filled squares) versus blend composition for mLLDPE/LDPE2 blends.

level of 20% (w/w) mLLDPE (see Fig. 10). On the basis of the radar plot areas associated with these figures, it can be shown that blends containing the LDPE2 material have overall superior properties than those containing the LDPE1. However, it should be noted that with regard to dart impact strength (i.e. the high-rate deformation test) the radar plots reveal the blends containing LDPE1 to be superior to those containing LDPE2. As expected, this observation supports the data previously presented in Fig. 6 where LDPE1 is shown to be consistently superior to LDPE2 in this regard.

The normalized areas associated with the radar plots for all blend compositions studied has been calculated and is presented in Fig. 11a and b for the mLLDPE/LDPE1 and mLLDPE/LDPE2 systems respectively. As expected, the normalized area increases with increasing mLLDPE content in each of the blends. The normalized MFR values for each of the blends have been superimposed on these plots and, as expected, the values decrease with increasing mLLDPE content in the blend (see Fig. 1b). Since a relative decrease in the normalized MFR parameter reflects a reduction in processability [19, 49] and an increase in the normalized radar area indicates an improvement in the overall film properties, then the point at which these two plots intersect will be indicative of a blend with optimal physicomechanical and optical properties as well as optimal processability. For blends of mLLDPE with LDPE1 (Fig. 11a), the optimal blend composition is ca. 30% (w/w) mLLDPE whereas for blends of mLLDPE with LDPE2 (Fig. 11b), the optimal blend composition is ca. 20% (w/w) mLLDPE.

4. Conclusions

Two series of film blends of mLLDPE with LDPE were prepared and the physicomechanical and optical properties were systematically and successfully studied. The

melt flow properties of these blends were also studied in order to assess the ease at which the blends can be processed. It was found that the addition of mLLDPE to LDPE improves most of the properties under consideration in this work and that the LDPE material having a higher polydispersity produces blends that have generally superior properties. A novel adaptation of conventional radar plots, involving the calculation of the area enclosed by the polygon on such a plot, enables one to identify a level at which mLLDPE can be incorporated in LDPE to produce optimal overall properties. In the case of the LDPE materials used in the current study, a level of mLLDPE of between 20–30% (w/w) appears to be that required to achieve optimization.

References

1. R. A. RUBECK and H. M. BAKER, *Polymer* **23** (1982) 1680.
2. G. D. WIGNALL, J. D. LONDONO, J. S. LIN, R. G. ALAMO, M. J. GALANTE and L. MANDELKERN, *Macromolecules* **28** (1995) 3156.
3. M. REE, T. KYU and R. S. STEIN, *J. Polym. Sci., B, Polym. Phys.* **25** (1987) 105.
4. J. I. IRAGORRI, J. M. REGO, I. KATIME, M. T. CONDE BRAÑA and U. W. GEDDE, *Polymer* **33** (1990) 461.
5. S. HOSODA, *Polym. J.* **20** (1988) 383.
6. L. A. HAMIELEC, *Polym. Eng. Sci.* **26** (1986) 111.
7. A. SIEGMANN and Y. NIR, *ibid.* **27** (1987) 1182.
8. F. M. MIRABELLA, JR. and E. A. FORD, *J. Polym. Sci., B, Polym. Phys.* **25** (1987) 777.
9. E. KARBASHEWSKI, L. KALE, A. RUDIN, W. J. TCHIR, D. G. COOK and J. O. PRONOVOST, *J. Appl. Polym. Sci.* **44** (1992) 425.
10. A. BARBALATA, T. BOHOSSIAN and G. DELMAS, *ibid.* **46** (1992) 411.
11. A. D. CHANNELL and E. Q. CLUTTON, *Polymer* **33** (1992) 4108.
12. F. M. MIRABELLA, JR., S. P. WESTPHAL, P. L. FERNANDO, E. A. FORD and J. G. WILLIAMS, *J. Polym. Sci., B, Polym. Phys.* **26** (1988) 1995.
13. A. D. CHANNELL, E. Q. CLUTTON and G. CAPACCIO, *Polymer* **35** (1994) 3893.
14. T. M. LIU and W. E. BAKER, *Polym. Eng. Sci.* **31** (1991) 751.
15. F. DEFOOR, G. GROENINCKX, P. SCHOUTERDEN and B. VAN DER HEIJDEN, *Polymer* **33** (1992) 3878.
16. D. M. KAYLON and F. H. MOY, *Polym. Eng. Sci.* **28** (1988) 1551.
17. D. L. WILFONG and G. W. KNIGHT, *J. Polym. Sci., B, Polym. Phys.* **28** (1990) 861.
18. L. E. BAILEY, D. G. COOK, J. PRONOVOST and A. RUDIN, *Polym. Eng. Sci.* **34** (1994) 1485.
19. M. A. SPALDING, D. E. KIRKPATRICK and K. S. HYUN, *ibid.* **33** (1993) 423.
20. A. C.-Y. WONG, *ibid.* **31** (1991) 1549.
21. C. S. SPEED, *Plast. Eng.* **July** (1982) 39.
22. S. HAGHIGHAT and A. W. BIRLEY, *Plast. Rubber Process. Appl.* **13** (1990) 197.
23. P. VADHAR and T. KYU, *Polym. Eng. Sci.* **27** (1987) 202.
24. A.J. MÜLLER, V. BALSAMO, F. DA SILVA, C. M. ROSALES and A. E. SÁEZ, *ibid.* **34** (1994) 1455.
25. B. TREMBLAY, *ibid.* **32** (1992) 65.
26. J. J. GUNDERSON and D. R. PARIKH, *ACS Div. Polym. Sci., Polym. Prepr.* **30** (1989) 233.
27. T. KYU, S.-R. HU and R. S. STEIN, *J. Polym. Sci., B, Polym. Phys.* **25** (1987) 89.
28. F. MARTINEZ and N. BARRERA, *Tappi J.* **74** (1991) 165.
29. J.-H. OH, *J. Reinf. Plast. Compos.* **18** (1999) 662.
30. K. TASHIRO, R. S. STEIN and S. L. HSU, *Macromolecules* **25** (1992) 1801.
31. A. PRASAD, *Polym. Eng. Sci.* **38** (1998) 1716.
32. M. YAMAGUCHI and S. ABE, *J. Appl. Polym. Sci.* **74** (1999) 3153.
33. K. M. DRUMMOND, J. L. HOPEWELL and R. A. SHANKS, *ibid.* **78** (2000) 1009.
34. Y.-T. SHIEH and H.-C. CHUANG, *ibid.* **81** (2001) 1808.
35. T. TSUKAME, Y. EHARA, Y. SHIMIZU, M. KUTSUZAWA, H. SAITOH and Y. SHIBASAKI, *Thermochim. Acta* **299** (1997) 27.
36. A. AJJI, P. SAMMUT and M. A. HUNEAULT, *J. Appl. Polym. Sci.* **88** (2003) 3070.
37. A. C.-Y. WONG and A. D. E. SY, *J. Mater. Sci.* **30** (1995) 5672.
38. J. A. PARKER, D. C. BASSETT, R. H. OLLEY and P. JAASKELAINEN, *Polymer* **35** (1994) 4140.
39. T. C. YU and G. J. WAGNER, SPE'RETEC Polyolefins VIII Conference (1993) .
40. J. C. W. CHIEN and D. HE, *J. Polym. Sci., A, Polym. Chem.* **29** (1991) 1585.
41. J. H. SCHUT, *Plast. World* **53** (1995) 12.
42. *Idem., ibid.* **53** (1995) 18.
43. R. D. LEAVERSUCH, *Mod. Plast. Int.* **70** (1995) 18.
44. C.-T. LUE, *J. Plast. Film Sheeting* **15** (1999) 131.
45. A. MAJUMDAR and D. D. KALE, *J. Appl. Polym. Sci.* **81** (2001) 53.
46. M. HESS, B. L. LOPEZ and C. GARTNER, *Macromol. Symp.* **174** (2001) 277.
47. C. LIU, J. WANG and J. HE, *Polymer* **43** (2002) 3811.
48. I. A. HUSSEIN, T. HAMEED, B. F. A. SHARKH and K. MEZGHANI, *ibid.* **44** (2003) 4665.
49. T. BREMNER, A. RUDIN and D. G. COOK, *J. Appl. Polym. Sci.* **41** (1990) 1617.
50. J. MINICK, A. MOET and E. BAER, *Polymer* **36** (1995) 1923.
51. D. R. RUEDA, F. J. BALTÁ-CALLEJA, A. VIKSNE and L. MALERS, *J. Mater. Sci.* **29** (1994) 1109.
52. H. UEDA, F. E. KARASZ and R. J. FARRIS, *Polym. Eng. Sci.* **26** (1986) 1483.
53. G. H. EDWARD, *Br. Polym. J.* **18** (1986) 88.
54. B. H. CLAMPITT, *Anal. Chem.* **35** (1963) 577.
55. J. LU, H.-J. SUE and T. P. RIEKER, *J. Mater. Sci.* **35** (2000) 5169.
56. Y.-M. KIM and J.-K. PARK, *J. Appl. Polym. Sci.* **61** (1996) 2315.

Received 20 May
and accepted 20 September 2004